



HAL
open science

Hierarchy Control of Dual-arm Concentric Tube Continuum Robots with Different Redundancy Resolution Techniques

Tarek Alsaka, Philippe Cinqun, M. Taha Chikhaoui

► **To cite this version:**

Tarek Alsaka, Philippe Cinqun, M. Taha Chikhaoui. Hierarchy Control of Dual-arm Concentric Tube Continuum Robots with Different Redundancy Resolution Techniques. *Advances in Robot Kinematics*, Jun 2024, Ljubljana, Slovenia. hal-04585876

HAL Id: hal-04585876

<https://hal.science/hal-04585876>

Submitted on 23 May 2024

HAL is a multi-disciplinary open access archive for the deposit and dissemination of scientific research documents, whether they are published or not. The documents may come from teaching and research institutions in France or abroad, or from public or private research centers.

L'archive ouverte pluridisciplinaire **HAL**, est destinée au dépôt et à la diffusion de documents scientifiques de niveau recherche, publiés ou non, émanant des établissements d'enseignement et de recherche français ou étrangers, des laboratoires publics ou privés.

Hierarchy Control of Dual-arm Concentric Tube Continuum Robots with Different Redundancy Resolution Techniques

Tarek Alsaka, Philippe Cinquin, and M. Taha Chikhaoui

Abstract Robot-assisted Single Port (SP) surgical systems have become popular in laparoscopy, consisting of multiple flexible instruments and an endoscope emerging through a single cannula. This innovative approach presents several challenges related to a smaller workspace and visual field of view. Previous works on Dual-Arm Concentric Tube Continuum Robots (DACTCR) aimed to enhance SP systems by increasing autonomy in a specific surgical subtask, thus simplifying procedures and reducing the surgeon's workload. This paper extends beyond state-of-the-art methods, particularly the utilization of the relative Jacobian and null-space projection for cooperation control. The main contributions of this paper in simulation involve the incorporation of an actuation limit avoidance solution as an additional block to the DACTCR control system and the evaluation of different promising redundancy resolution techniques like saturation in the null-space and null-space projection, both formulated as constrained quadratic programming problems.

1 Introduction

Robot-assisted single port surgery has become a trend in the last decade due to the major benefits to patients with less invasiveness and faster recovery [1]. On the other hand, it poses more technological challenges, especially the need for flexible and miniaturized instruments. This flexibility requires more active management and frequent adjustments by the surgeon to maintain an optimal view of the surgical site when manipulating the endoscopic camera, while having to control two other instruments for instance. Consequently, the workload on the surgeon tends to be high [2]. The need for precise instrument control and constant visual monitoring can be demanding, underscoring the importance of surgeon expertise in SP surgery. Continuum Robots (CR) have been used as SP systems with outer diameters ranging from 12 to 25 *mm* (see Fig. 1). They consider a joint-less structure in contrast to a

Tarek Alsaka, Philippe Cinquin, and M. Taha Chikhaoui
Univ. Grenoble Alpes, CNRS, UMR 5525, VetAgro Sup, Grenoble INP, TIMC, 38000 Grenoble, France, e-mail: firstname.lastname@univ-grenoble-alpes.fr

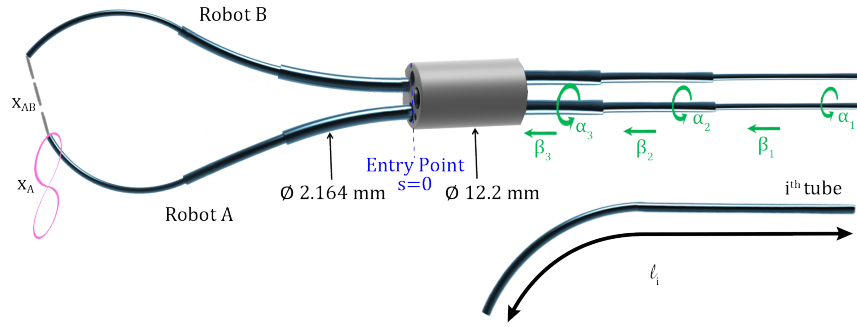


Fig. 1: A DACTCR schematic inserted in a dual-channel endoscope. The active part of the robot starts at the entry point $s = 0$. The pink line denotes a potential end-effector desired trajectory x_A while the gray line is the relative position x_{AB} . $\beta_i < 0$ is the distance of the end of tube i from $s = 0$ and refers to translation actuation, while α_i is the rotation actuation of each tube.

conventional manipulator consisting of rigid links connected by joints in which the independent joints define the Degrees of Freedom (DoF) of the robot. Hence, CR are classified as robots with *infinite DoF*. Considering the high safety requirements for surgery, most surgical robots are still at level 1 of autonomy [3]. That means surgeons using a console have full control over the robot through **teleoperation**. Increasing the level of robot autonomy by enabling it with routine tasks is a promising research direction. In terms of the control approaches, Damped-Least Squares and Differential Inverse-Kinematics (DLS-DIK) have been mostly exploited as by Burgner et al. [4] for a DACTCR. In simulation, the work of Chikhaoui et al. [5] brought the idea of relative Jacobian already employed on serial manipulators [6] to CR class. This approach allows for the use of DIK in controlling a dual-arm as one structure. Also, null-space projection is utilized for hierarchy control, enabling automated **cooperation** tasks between the instruments. Later, Zhang et al. [7] built their work upon [5] to validate the controller in a real prototype of DACTCR. Such frameworks can be further improved. First, the control algorithm has been tested for specific scenarios where the initial configurations of the dual-arm have been identical, which may not be the case in real scenarios. Therefore, any deviation from this condition can impact the task performance. Second, they lack an actuation limit avoidance technique at the proximal part of the Concentric Tube Continuum Robot (CTCR), which is critical to avoid damage of the system. Bruns et al. [8] have developed a SP system with three CTCR and a robotic endoscope arm. They used DLS-DIK with a weighted cost function [9] to solve for actuation limit and elastic instability avoidance while teleoperating one robot. Shen et al. [10] exploited the same technique for actuation limit avoidance in a null-space projection scheme to achieve trajectory tracking while maximizing the manipulability for one CTCR. Our current work builds upon these major advances to propose the following contributions

- Incorporating weighted least norm solution into a null-space projection scheme for DACTCR to solve for actuation limit avoidance.
- Evaluating different redundancy resolution techniques to control the DACTCR like Saturation in the Null-Space (SNS), as well as exploiting the null-space projection formulated as constrained quadratic programming (QP).

2 Control Methods

Without loss of generality, this paper studies the following three tasks. First, to control the relative position of the DACTCR end-effectors denoted $x_{AB} \in \mathbb{R}^m$, where m is the task space dimension (3 for position control in our case). Second, trajectory tracking by the end-effector of robot A denoted $x_A \in \mathbb{R}^m$. Third, actuation limit avoidance. The actuation space of the CTR is $q = [\beta_1, \dots, \beta_n, \alpha_1, \dots, \alpha_n]^T \in \mathbb{R}^{2n}$, where n is the number of tubes. The rotational actuators α_i are independent, while the translational ones are related by the following proximal constraint [11]:

$$\begin{aligned} \beta_1 &\in [-\ell_1, 0] \\ \beta_n &\in [\max(-\ell_n, \beta_{n-1}), \min(\beta_{n-1} + \ell_{n-1} - \ell_n, 0)] \end{aligned} \quad (1)$$

Here, ℓ_i is the tube length (see Fig. 1). Note that these proximal constraints enforce distal constraints, i.e. the inner tube cannot be completely retracted into the outer one in the active part of the robot. The relation between the end-effector velocities \dot{x}_{AB} of the DACTCR and actuation velocities is described by

$$\dot{x}_{AB} = J_{AB} \dot{q}_{AB} = J_{AB} [\dot{q}_A \ \dot{q}_B]^T \quad (2)$$

where $\dot{q}_{AB} \in \mathbb{R}^{n_A+n_B}$ are the actuator velocities of the DACTCR ($n_A = n_B = 6$ for three-tubes CTR denoted A and B, respectively). $J_{AB} \in \mathbb{R}^{m \times (n_A+n_B)}$ is the relative Jacobian matrix constituted from the individual Jacobian matrices $J_A \in \mathbb{R}^{m \times n_A}$ and $J_B \in \mathbb{R}^{m \times n_B}$ of robots A and B, respectively. Since $n_{A/B} > m$, the robot is kinematically redundant and the closed-loop control law based on DIK and the null-space projection is given by

$$\dot{q}_{AB} = J_{AB}^\dagger v_{AB} + N_{AB} \nabla F_2(q_A) \quad (3)$$

where $v_{AB} = \lambda_{AB} \epsilon_{AB}$ is the desired primary task velocity, λ_{AB} is the control gain, $\epsilon_{AB} \in \mathbb{R}^3$ is the relative position error, J_{AB}^\dagger refers to the pseudo-inverse of J_{AB} and $N_{AB} = (I_{12} - J_{AB}^\dagger J_{AB})$ is the null-space projection of the robot's relative Jacobian matrix J_{AB} . $\nabla F_2(q_A) = J_A^\dagger v_A$ is the gradient of the secondary task, which is to control robot A to follow the desired trajectory, where $v_A = \lambda_A \epsilon_A + \dot{x}_A^d$ is the desired secondary task velocity, λ_A is the control gain, $\epsilon_A \in \mathbb{R}^3$ is the position error, and \dot{x}_A^d is trajectory feed-forward term of robot A. In order to perform the described tasks, we study three different control methods.

2.1 Null-Space Projection with Weighted Least Norm (NSPWLN)

When executing a task like trajectory tracking $x \in \mathbb{R}^m$, Chan and Dubey [9] proposed a weighted least norm solution for actuation limit avoidance in standard manipulators. This solution minimizes $\dot{q}^T W_{\text{act.lim}} \dot{q}$ subject to the constraint $x = J\dot{q}$, where $W_{\text{act.lim}}$

is a diagonal positive definite weighting matrix. We adapt this solution for DACTCR by setting $W_{\text{act.lim}} = \text{diag}([\lambda_t w_1, \lambda_t w_2, \lambda_t w_3, \lambda_r, \lambda_r, \lambda_r])$. We choose to penalize translation actuation close to exceeding the limit and to relax rotation actuation, with $\lambda_t = 30$ and $\lambda_r = 1e^{-3}$. The elements $w_i = 1 + \left| \frac{\partial H(\beta)}{\partial \beta_i} \right|$, where $H(\beta)$ is a performance criterion function (further details in [9]). To incorporate this solution in a dual-arm control scheme, we minimize two cost functions that include the weighted norm for actuation limit avoidance in each hierarchy level as follows

$$F_1(q_{AB}) = \frac{1}{2} (J_{AB} \dot{q}_{AB} - v_{AB})^T W_{\text{track.}} (J_{AB} \dot{q}_{AB} - v_{AB}) + \dot{q}_{AB}^T W_{\text{act.lim.}} \dot{q}_{AB} \quad (4)$$

$$F_2(q_A) = \frac{1}{2} (J_A \dot{q}_A - v_A)^T W_{\text{track.}} (J_A \dot{q}_A - v_A) + \dot{q}_A^T W_{\text{act.lim.A}} \dot{q}_A \quad (5)$$

where $W_{\text{track.}} = \text{diag}([1e^8, 1e^8, 1e^8, 0, 0, 0])$ is fine-tuned to these values, in which a higher value makes the corresponding tracking error more critical in the cost function. Then, the instantaneous actuation velocities for both tasks is

$$\dot{q}_{AB} = \underbrace{\left[\begin{array}{c} \underbrace{\left(J_{AB_{\text{left}}}^T W_{\text{track.}} J_{AB_{\text{left}}} + W_{\text{act.lim.A}} \right)^\dagger J_{AB_{\text{left}}}^T W_{\text{track.}}}_{\text{inv}(J_{AB})} \\ \underbrace{\left(J_{AB_{\text{right}}}^T W_{\text{track.}} J_{AB_{\text{right}}} + W_{\text{act.lim.B}} \right)^\dagger J_{AB_{\text{right}}}^T W_{\text{track.}}}_{\text{inv}(J_{AB})} \end{array} \right]}_{\nabla F_1(q_{AB})} v_{AB} + N_{AB} \underbrace{\left(J_A^T W_{\text{track.}} J_A + W_{\text{act.lim.A}} \right)^\dagger J_A^T W_{\text{track.}} v_A}_{\nabla F_2(q_A)} \quad (6)$$

where $N_{AB} = [I_{12 \times 12} - \text{inv}(J_{AB}) J_{AB}]$ is the new projection matrix, $J_{AB_{\text{left}}}/J_{AB_{\text{right}}}$ are the first/last six columns of J_{AB} , respectively. Note that the vectors and matrices are padded with zeros when necessary.

2.2 Null-Space Projection formulated as constrained Quadratic Programming (NSPQP)

The null-space projection given by (3) analytically solves the primary task in a least-squares sense while minimizing the distance to the secondary task gradient, $\nabla F_2(q_A)$. This problem can be formulated as constrained QP with both equality and inequality constraints, expressed as

$$\begin{aligned} \min_{\dot{q}_{AB}} \quad & \frac{1}{2} \dot{q}_{AB}^T \left(J_A^T J_A + \zeta I \right) \dot{q}_{AB} - v_A^T J_A \dot{q}_{AB} \\ \text{s.t.} \quad & J_{AB} \dot{q}_{AB} = v_{AB}, \quad \dot{Q}_{\min} \leq \dot{q}_{AB} \leq \dot{Q}_{\max} \end{aligned} \quad (7)$$

where ζ is a regularization parameter. The lower and upper bounds on \dot{q}_{AB} , denoted \dot{Q}_{\min} and \dot{Q}_{\max} respectively, are computed as per the method described in [12]:

$$\dot{Q}_{\min,i} = \max \left\{ \frac{\beta_{\min,i} - \beta_i}{T}, -\mathcal{V}_{\max,i}, -\sqrt{2\mathcal{A}_{\max,i} (\beta_i - \beta_{\min,i})} \right\}$$

$$\dot{Q}_{max,i} = \min \left\{ \frac{\beta_{max,i} - \beta_i}{T}, \mathcal{V}_{max,i}, \sqrt{2\mathcal{A}_{max,i} (\beta_{max,i} - \beta_i)} \right\}$$

Here, $\beta_{min,i}$ and $\beta_{max,i}$ from (1) are the lower and upper bounds for tube i and T is the control sampling time. $\mathcal{V}_{max,i}$ and $\mathcal{A}_{max,i}$ represent the maximum velocity and acceleration for the translation actuation, respectively. Notably, the rotational components of \dot{q}_{AB} remain unbounded.

2.3 Saturation in the Null-Space formulated as constrained Quadratic Programming (SNSQP)

The SNS algorithm [12] is a robust redundancy resolution technique to analytically solve the DIK while preserving the hard actuation limit constraints during the execution of prioritized tasks. In essence, the approach involves saturating the most overdriven actuation one at a time if one or more actuators exceed their limits. The contribution of this actuation is then reintroduced into the null-space of a suitable Jacobian matrix until a feasible solution is found, all without affecting the task execution. Furthermore, SNS incorporates the selection of a task scaling factor, ensuring the execution of the task direction with minimal scaling for tasks that may not be feasible. The equivalent QP problem is formulated as follows

$$\begin{aligned} \min_{\dot{q}_{AB}, s_k} \quad & \frac{1}{2} \dot{q}_{AB}^T (\zeta \mathbf{I}) \dot{q}_{AB} + \frac{1}{\zeta} (1 - s_k)^2 \\ \text{s.t.} \quad & \mathbf{J}_k \dot{q}_{AB} = s_k v_k, \quad \mathbf{J}_{1 \rightarrow k-1} \dot{q}_{AB} = \mathbf{J}_{1 \rightarrow k-1} \dot{q}_{AB_{k-1}}, \quad \dot{Q}_{min} \leq \dot{q}_{AB} \leq \dot{Q}_{max} \end{aligned} \quad (8)$$

Here, s_k is task scale factor, \mathbf{J}_k is the current Jacobian, v_k is the desired task, and $\mathbf{J}_{1 \rightarrow k-1}$ is the stack of the Jacobian of the higher-priority tasks. The parameter ζ serves as a trade-off between minimum actuation velocity and maximum task scale.

3 Simulation results

In the subsequent results, the CTCR design parameters specified in Table 1 are used for both robots. These parameters are used for an experimental setup in the lab. To

Table 1: Tube design parameters

Tube #	1	2	3
ϕ_{out} / ϕ_{in} (mm)	1.524/1.3	1.8/1.62	2.164/2
E (GPa)	58	58	58
ν	0.6	0.6	0.6
L_s (mm)	387	267	149
L_c (mm)	50	50	50
κ (mm^{-1})	0.1	0.05	0.07

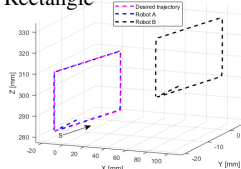
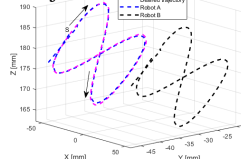
ϕ_{out} / ϕ_{in} : outer and inner diameters, E : Young's modulus, ν : Poisson ratio, L_s and L_c are the tube's straight and curved lengths, respectively, and κ : curvature.

Table 2: Initial configurations for the control simulations

q	Config 1		Config 2		Config 3	
	A	B	A	B	A	B
β_1 (mm)	-100	-80	-150	-130	-250	-250
β_2 (mm)	-80	-60	-100	-120	-200	-200
β_3 (mm)	-50	-30	-50	-100	-120	-120
α_1 (°)	45	45	180	90	0	0
α_2 (°)	45	45	90	-60	0	0
α_3 (°)	45	45	45	-270	0	0

validate the control algorithm, we arbitrarily select different initial configurations, as outlined in Table 2. These configurations encompass varied initial relative positions for the primary task, which is held constant during the trajectory tracking. The evaluation involves testing two types of trajectories, Rectangle and Lissajous, starting off the end-effector location. For each point along the trajectory, we run an internal control loop with a maximum of 100 iterations or converging to a predefined threshold of 0.88 mm before advancing to the next point. All methods are executed with a sampling time $T = 0.1 \text{ s}$ and identical task gains, where $\lambda_{AB} = 5$ and $\lambda_A = 3$. In the cases of NSPQP and SNSQP, both the maximum velocity \mathcal{V}_{max} and acceleration \mathcal{A}_{max} are set to 5 mm/s and 1 mm/s^2 , respectively. Table 3 provides a comparison of control errors among the three methods. All successfully converge within the specified threshold. Notably, the NSPQP and SNSQP demonstrate comparable performances, exhibiting the lowest errors ranging from 0.02 to 0.13 mm (as maximum) for the primary task and 0.74 to 0.82 mm (as maximum) for the secondary one. The NSPWLN closely follows, displaying competitive performances with maximum errors of 0.35 and 0.82 mm , respectively. However, this latter method requires almost as twice more iterations as the others and, more importantly, fails to respect the actuation limit in one case, as depicted in Fig. 2. Finally, a trade-off exists between achieving a minimum norm velocity and maximizing task scaling in SNSQP. This presents an advantageous feature wherein, if the robot approaches a nearly infeasible region within the workspace, task scaling can facilitate task completion by reducing the task velocity. In contrast, in NSPQP, the controller fails to adapt under similar circumstances unless one manually re-tunes the task gain to a suitable value.

Table 3: Control errors for the three methods

Trajectory	Method	Iterations	RMS \pm StD [Max] (mm)
	NSPWLN	523	$\epsilon_{AB}: 0.33 \pm 0.05 [0.35]$ $\epsilon_A: 0.79 \pm 0.08 [0.82]$
	NSPQP	269	$\epsilon_{AB}: 0.01 \pm 0.02 [0.02]$ $\epsilon_A: 0.72 \pm 0.10 [0.81]$
	SNSQP	261	$\epsilon_{AB}: 0.02 \pm 0.03 [0.05]$ $\epsilon_A: 0.70 \pm 0.11 [0.74]$
	NSPWLN	513	$\epsilon_{AB}: 0.31 \pm 0.04 [0.33]$ $\epsilon_A: 0.78 \pm 0.07 [0.81]$
	NSPQP	279	$\epsilon_{AB}: 0.03 \pm 0.04 [0.09]$ $\epsilon_A: 0.72 \pm 0.10 [0.75]$
	SNSQP	259	$\epsilon_{AB}: 0.06 \pm 0.08 [0.13]$ $\epsilon_A: 0.71 \pm 0.10 [0.76]$

ϵ_{AB} : Relative end-effector positioning error, ϵ_A : Trajectory tracking error with end-effector A. Each row is the average value of the three different initial configurations in Table 2.

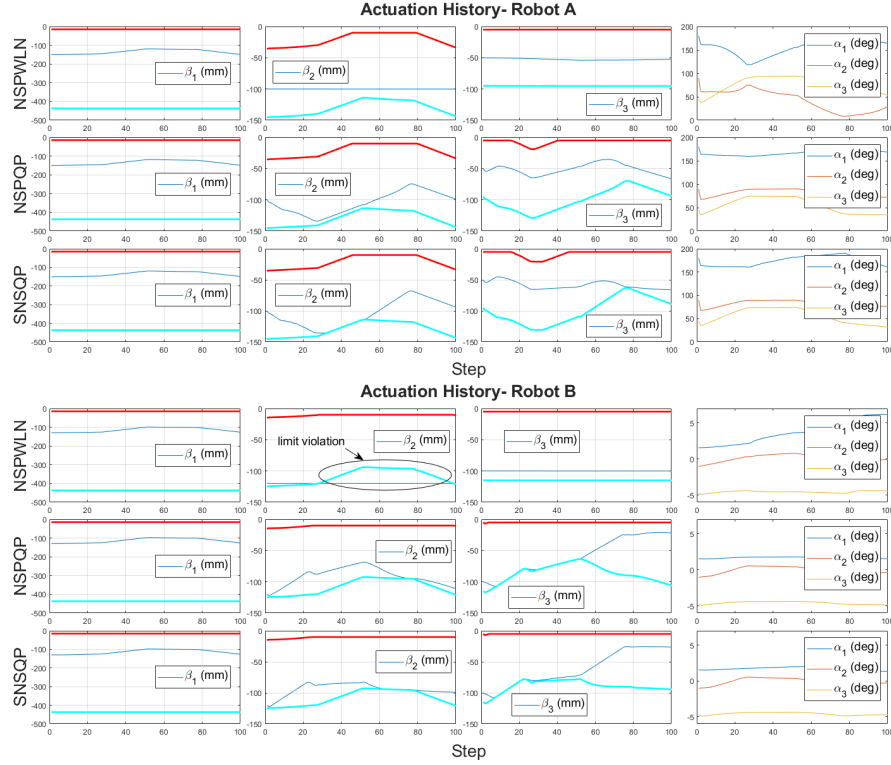


Fig. 2: Actuation history comparison for robots A (top) and B (bottom) across three methods (each in a row), with red and cyan representing upper and lower bounds of the translation actuation. The actuation limit boundary of (1) includes additional small thresholds to ensure minimum segment length and spacing between the motors within the actuation unit. Each step represents a trajectory point.

4 Discussion and future work

Incorporating actuation limit avoidance into any control algorithm is essential, especially in situations where the robot's actuation space is significantly constrained, as is the case in CTCR. However, as observed in the comparison of the three methods studied in this paper, addressing this issue results in distinct robot behaviors. For instance, in the NSPWLN control algorithm, we note a dependency on rotational actuation while restricting the translational actuation of the tubes. This causes some tubes to remain nearly unextended, creating difficulties in avoiding the actuation limit since the controller is not aware about the movement of other tubes. Therefore, a future work would be to find a more suitable cost function to overcome this limitation. In opposite, the other two methods allow more freedom in tube movement, enabling acceleration or deceleration before reaching the limit and smoothly repulsing the system from the limit when necessary. Such performances could be significant,

particularly in medical applications where operational space is highly limited, and safety requirements are paramount. In scenarios demanding limited tube translation, the NSPWLN solution may be preferable. On the other hand, controlling the tube's velocity, as provided by the two QP methods, holds importance for the safety as well. Hence, there exists a trade-off between minimizing tube translation and controlling tube velocity, all while ensuring the feasible actuation limits and guaranteeing task accomplishment. Further exploration of real environments is planned to determine the optimal control method. Finally, we plan to conduct experimental validation on a DACTCR prototype to assess the control performances in real scenarios, taking into account for example the sensor accuracy, actuator resolution, and potential elastic instability of the robot prototype.

Acknowledgments

This work is supported by grants ANR-20-CE33-0001 and ANR-11-LABX-0004-01.

References

1. K. Khandalavala, T. Shimon, L. Flores, P. R. Armijo, and D. Oleynikov. Emerging surgical robotic technology: a progression toward microbots. *Annals Laparoscopic and Endoscopic Surgery*, 5(0), 2019.
2. H. Norasi, E. Tetteh, K. E. Law, S. Ponnala, M. S. Hallbeck, and M. Tollefson. Intraoperative workload during robotic radical prostatectomy: Comparison between multi-port da vinci xi and single port da vinci sp robots. *Appl. Ergon.*, 104:103826, 2022.
3. T. Haidegger. Autonomy for surgical robots: Concepts and paradigms. *IEEE Trans. Med. Robot. Bionics.*, 1(2):65–76, 2019.
4. J. Burgner-Kahrs, P. J. Swaney, D. C. Rucker, H. B. Gilbert, S. T. Nill, P. T. Russell, K. D. Weaver, and R. J. Webster. A bimanual teleoperated system for endonasal skull base surgery. In *IEEE/RSJ Int. Conf. Intelligent Robot. Sys.*, pages 2517–2523, 2011.
5. M. T. Chikhaoui, J. Granna, J. Starke, and J. Burgner-Kahrs. Toward motion coordination control and design optimization for dual-arm concentric tube continuum robots. *IEEE Robot. Autom. Letters*, 3(3):1793–1800, 2018.
6. R. S. Jamisola and R. G. Roberts. A more compact expression of relative jacobian based on individual manipulator jacobians. *Robot. Auton. Syst.*, 63:158–164, 2015.
7. H. J. Zhang, S. Lilge, M. T. Chikhaoui, and J. Burgner-Kahrs. Cooperative control of dual-arm concentric tube continuum robots. In *MARSS*, pages 1–6, 2022.
8. T. L. Bruns, A. A. Ramirez, M. A. Emerson, R. A. Lathrop, A. W. Mahoney, H. B. Gilbert, C. L. Liu, P. T. Russell, R. F. Labadie, K. D. Weaver, and III R. J. Webster. A modular, multi-arm concentric tube robot system with application to transnasal surgery for orbital tumors. *Int. J. Robot. Res.*, 40(2-3):521–533, 2021.
9. T. F. Chan and R. V. Dubey. A weighted least-norm solution based scheme for avoiding joint limits for redundant joint manipulators. *IEEE Tran. Robot. Autom.*, 11(2):286–292, 1995.
10. J. Shen, Y. Wang, M. Azizkhani, D. Qiu, and Y. Chen. Concentric tube robot redundancy resolution via velocity/compliance manipulability optimization. *arXiv:2305.06194*, 2023.
11. J. Burgner-Kahrs, H. B. Gilbert, J. Granna, P. J. Swaney, and R. J. Webster. Workspace characterization for concentric tube continuum robots. In *IEEE/RSJ Int. Conf. Intelligent Robot. Sys.*, pages 1269–1275, 2014.
12. F. Flacco, A. De Luca, and O. Khatib. Control of redundant robots under hard joint constraints: Saturation in the null space. *IEEE Trans. Robot.*, 31(3):637–654, 2015.